Pure Appl. Geophys.

https://doi.org/10.1007/s00024-019-02196-2

Pure and Applied Geophysics

Pros and Cons in Helicopter-Borne GPR Data Acquisition on Rugged Mountainous Areas: Critical Analysis and Practical Guidelines

E. Forte,[1] M. Basso Bondini,[1] A. Bortoletto,[2,3] M. Dossi,[1] and R. R. Colucci[4]

Abstract—We critically discuss both advantages and limitations of helicopter-borne GPR surveys in rugged mountainous areas by analyzing a pseudo 3D data set acquired over the Marmolada Glacier, which constitutes the largest ice body in the Dolomites (Eastern Alps) and contains several peculiar features both in terms of the internal structures and the surrounding topography. In this paper we analyze several possible issues that can be encountered when performing airborne surveys in mountain regions, related to both the local conditions in the particular survey areas, and the general performance of the data acquisition equipment, which includes the GPR device, the GPS system, and the helicopter itself. Based on our analyses and observations, we propose a few guidelines and optimization strategies in order to address several issues, including the choice of various data acquisition parameters, interpretation problems related to curvilinear or irregular flight paths, and trace positioning errors caused by GPS malfunctioning or oscillating antennas. Such results have general validity and can be used for helicopter-borne survey planning, as well as for data analysis and interpretation.

Key words: Helicopter-borne GPR, GPR surveys, GPR data acquisition, rugged mountainous area, limitations, GPR parameters.

1. Introduction

Ground Penetrating Radar (GPR) is a non-invasive near-surface geophysical technique based on the propagation of high frequency (typically in the 10 MHz–2 GHz range) electromagnetic (EM) waves in the subsurface. Since the signal propagation is mainly affected by the EM properties of the ground, GPR data sets can be used to study the subsurface materials and structures (Jol 2009) with varying degrees of resolution and penetration. At present, GPR systems are used in a plethora of applications in several fields, including archeology, geology, engineering, hydrology, glaciology, and many others (Daniels 2004; Jol 2009), even for time monitoring purposes (Birken et al. 2000; Truss et al. 2007; Forte et al. 2014) mainly thank to the higher versatility, resolution, and acquisition rates, when compared to any other geophysical technique.

Most GPR surveys are performed using ground-coupled systems, in which the antennas are placed either directly on the ground surface or just a few centimeters above it, and are moved across the survey area manually or using vehicles. However, ground-based GPR surveys may face significant logistical challenges posed by rough terrain, especially in remote locations, as well as safety concerns due for instance to the possible presence of crevasses, or the risk of landslides and avalanches. In these conditions, airborne GPR surveys may be preferable, since they are less affected by terrain challenges, thus allowing to safely operate even in otherwise dangerous locations (Rutishauser et al. 2016). In addition, these techniques can be used to rapidly survey large areas, potentially covering several tens of kilometers per hour, which can be compared only to few other specific applications, such as asphalt pavement inspection and thickness mapping (Khamzin et al. 2017), in which GPR antennas mounted on vehicles allow to perform high-speed surveys. Despite such advisable advantages of remote GPR surveying, nowadays airborne applications are not as widespread and well-developed as their counterparts, the

[1] Department of Mathematics and Geosciences, University of Trieste, via Edoardo Weiss, 1, 34128 Trieste, TS, Italy. E-mail: eforte@units.it

[2] *Present Address*: Fugro, Prismastraat 4, 2631 RT Nootdorp, South Holland, The Netherlands.

[3] Helica srl, via Fratelli Solari10, 33020 Amaro, UD, Italy.

[4] Department of Earth System Sciences and Environmental Technologies, ISMAR-CNR Trieste, Area Science Park, Q2 building, S.S. 14, km 163.5, 34149 Basovizza, TS, Italy.

Published online: 26 April 2019

conventional ground coupled antennas (Cabrera and Bekic 2018). On the other hand, airborne surveys have been performed for a long time using Radio Echo Sounding (RES) systems (Steenson 1951; Cook 1960; Watte and Schmidt 1962; Evans and Robin 1966), which are similar in principle to commercial GPR (Arcone et al. 1995). A comprehensive review of such equipment, which is not the focus of this paper, is provided for instance by Plewes and Hubbard (2001).

The quality of airborne data sets can nevertheless be limited by the mobility and logistical constraints of the aircraft. In particular, planes have a minimum flight speed, need a quite large area for turnarounds, and require runways for takeoffs and landings, which also necessitate additional facilities. Mainly for these reasons, surveys involving fixed wing aircrafts are limited to wide and relatively flat areas like in the Antarctic continent (Vaughn et al. 1999). For example, airborne RES surveys are one of the main prospecting tools used in Antarctica for ice sheet exploration and ice-bedrock interface detection, where the ice column can exceed 4 km in thickness (Urbini et al. 2017).

Nowadays, most airborne GPR surveys are performed using helicopters, which allow to cover large areas in a reasonably short period of time and with limited logistical demands. In fact, the high agility of helicopters allows to follow more complex and tortuous paths, with the possibility to increase the data density in areas of special interest. A few recent applications of GPR surveys conducted by hanging the antennas from a low-flying helicopter for archaeological purposes have been cited by Conyers (2013) and Gundelach et al. (2010), without further details. Blindow et al. (2011) provided some examples of geological applications, while Melcher et al. (2002) analyzed GPR data acquired from helicopter for hydrological purposes, and Lambot et al. (2006) did an interesting theoretical analysis about the possible use of air-launched GPR surveys to measure soil surface water content, which was partially applied by Jadoon et al. (2015). Fu et al. (2014) claim that airborne GPR has the potential to be expanded into broader applications, such as geohazard monitoring and investigations in desert environments, but, as far as we know, no relevant practical applications in these sectors have so far been reported in the scientific literature. A possible broadening of airborne GPR applications could arise by exploiting systems connected to small Unmanned Aerial Vehicle (UAV), as recently tested by Fasano et al. (2017) and Cabrera and Bekic (2018).

Nevertheless, airborne glaciological surveys are quite common, because they exploit the generally low electrical conductivity of frozen materials to reach penetration depths that are not possible for most geological materials. Signal penetration in GPR surveys can be limited by several factors, including spreading losses due to wavefront expansion, intrinsic attenuation, signal scattering, and partial reflections. For airborne surveys, the antenna elevation increases the distance traveled by the recorded signals with respect to ground-based surveys, leading to higher spreading losses. In terms of intrinsic attenuation, snow- and ice-covered surfaces are more favorable for airborne GPR surveys due to the aforementioned low conductivity, which can increase only when a significant amount of free (i.e. unfrozen) water is entrapped within or lies just above the frozen mass (Bradford et al. 2009; Godio 2009). In such circumstances, the attenuation of the EM signal when travelling through frozen materials is still usually very low when compared to most of the other geological media. In terms of partial reflections, the large reflection arising from the topographic surface can greatly reduce the signal energy, due to the significant EM impedance contrast between the air and ground materials. However, such contrast is significantly smaller when the survey area is covered by snow and ice, as opposed to outcropping rocks or sediments. Considering a normal incidence of a plane wave on a flat reflector, with both the electrical conductivity and magnetic permeability being negligible, the reflection coefficient (R_i) is given by the following relation:

$$R_i = \frac{\sqrt{\varepsilon_{ri}} - \sqrt{\varepsilon_{ri+1}}}{\sqrt{\varepsilon_{ri}} + \sqrt{\varepsilon_{ri+1}}} \quad (1)$$

The relative electrical permittivity (ε_r) of frozen materials is quite low, with values close to 1 for fresh snow and a maximum value of 3.2 for pure ice (e.g. Godio 2009; Forte et al. 2013). Therefore, since ε_r is equal to 1 in air, the reflection coefficients of ice-covered surfaces is equal to about -0.28 (Eq. 1),

which is almost half the value obtained from rocky surfaces, with ε_{r+1} equal to 10 in Eq. 1. Similar results arise when considering the power loss caused by the reflection, which is equal to $|R^2|$ when expressed in dB.

Besides the pioneering works of the last century, there are many examples of airborne GPR surveys used for mapping ice in different environments (Siegert et al. 2004; Gabbi et al. 2012; Rückamp and Blindow 2012; Gacitúa et al. 2015; Rutishauser et al. 2016) and monitoring snow accumulation (Machguth et al. 2006; Negi et al. 2008). More specific applications in frozen environments include permafrost studies (Arcone 2002), rock glaciers imaging (Merz et al. 2015a, b), and even peculiar issues like locating oil spills under the snow cover (Bradford et al. 2010). However, quite surprisingly, a recent review by Rutishauser et al. (2016) revealed that airborne GPR data sets are still rarely used to determine the thickness or the volume of temperate alpine glaciers. In addition, such surveys are often performed just on the larger and relatively flat glaciers within the valleys. In any case, it is worthy to remark that not all contractors are willing to show their survey results, and in many cases geophysical companies consider data strictly confidential. Extensive ground and airborne based GPR data sets were recently made available from government agencies (O'Neel et al. 2018).

In this paper, we focus on helicopter-borne GPR surveys performed on rough topography typical of many mountain glaciers, which do not always exhibit a smooth surface and are often relatively small and fragmented. These surveys are indeed important because mountain glaciers are so numerous in some areas that, at a regional scale, they can contain a significant fraction of ice volume, which must be taken into account in order to obtain meaningful global estimations (Bahr and Radić 2012; Pfeffer et al. 2014). Such data are in turn necessary for reliable mass balance estimations, water equivalent assessments, and for both short and long term forecasts. Moreover, in the near future, due to global warming, several cirque glaciers and small ice caps will be divided in separated smaller fractions, while the topography will become more complex and rugged due to differential melting. This is particularly true when glaciers lie on limestone lithologies, which exhibit not homogeneous water drainage.

Several works have addressed the performance of specific airborne GPR systems (Blindow et al. 2011; Krellmann and Triltzsch 2012), the comparison between ground- and air-based equipments (Rutishauser et al. 2016), as well as processing algorithms specifically dedicated to air-coupled antennas (Sen et al. 2003; Catapano et al. 2012), however less effort has been spent on critically analyzing possible problems and limitations related to remote GPR data acquisitions. Therefore, in this paper we concentrate on the two following issues:

1. Critical evaluation and discussion of the helicopter-borne data acquisition on rough terrains, with the aim of highlighting the main pros and cons;
2. Proposition of practical guidelines and possible optimization strategies to be applied during field data acquisitions in rugged mountainous areas.

In this light it is interesting to notice that a very recent paper of Cabrera and Bekic (2018) points out that GPR airborne systems often operate in very inefficient ways, sometimes disregarding basic physical laws and fundamental principles of GPR technology. Most of the problems are related to the antenna lifting from the topographic surface because a new set of complexities arise and, if not properly considered, they can lead to very unreliable data and consequent wrong interpretation.

Current airborne GPR systems can be classified into two main categories. The first one encompasses conventional commercial GPR antennas which are simply mounted under a helicopter; while the second one involves special hardware and antennas specifically developed for airborne surveys. Besides some obvious differences, it was recently reported that the two types of airborne GPR systems produce comparable results (Merz et al. 2015a; Rutishauser et al. 2016) in term of the overall attainable information. On the other hand, when comparing them to ground-based surveys, while Merz et al. (2015a) conclude that airborne data quality outperforms the one of ground-based data sets, Rutishauser et al. (2016) obtain opposite results. Nevertheless, both articles stress that the performance of each GPR system is

strongly site-specific, thus making the comparison overall inconclusive and preventing a priori recommendations of an optimal data acquisition method. Given the previous discussion, our focus on helicopter-borne GPR data sets can be considered paradigmatic in order to analyze possible issues arising when the survey area is characterized by rough topography, heterogeneous surface materials, and rapidly changing EM properties.

2. *Survey Area and GPR Data Acquisition*

We analyzed an 83 km long helicopter-borne GPR data set acquired on June 5th 2015 by Helica srl above the Marmolada Glacier, located in the Eastern Alps, Italy (Fig. 1). The Marmolada glacier is the largest ice body in the Dolomites (Eastern Alps) and it originates high on the northern side of the Marmolada massif (Punta Penia, 3343 m a.s.l., Figure 1) descending only part of the way to the main valley (hanging glacier). The glacier has approximate maximum width and length respectively equal to 3 and 1 km, with an estimated area of 1.67 km^2 in 2009 (Crepaz et al. 2010). The glacier develops between 2635 and 2935 m a.s.l., with a maximum thickness estimated in 2009 equal to 52 m (Crepaz et al. 2010). The oldest available data come from 1888, when the glacier supposedly had an area of 4.95 km^2 and had already slightly retreated from the Little Ice Age (LIA) maximum. Since the LIA, the Marmolada glacier has undergone an important reduction, similarly to all the other Italian Alpine glaciers (Salvatore et al. 2015; CGI 1978–2010). According to the most recent inventory, the Marmolada glacier is now divided into 7 smaller units (Smiraglia and Diolaiuti 2015). From a geomorphological point of view, this glacier represents an interesting case study, since it condenses many of the typical characteristics of alpine glaciers. In particular, the accumulation area of the main Marmolada glacier (ID CGI 941) is directly fed by precipitation but the mass balance is also partly influenced by avalanches in the western-most part. In this area, the glacier below the Punta Penia peak is called the Central Marmolada glacier (ID CGI 941.1) and, being virtually separated by the rest of the ice body, it might be considered as a cirque glacier (Smiraglia and Diolaiuti 2015). The presence of crevasses, although diminished in the last decade, is still important in some sectors. The highest portion of the Marmolada massif is characterized by the glacier of Punta Penia (ID CGI 941.2), which is a small ice cap close to the Punta Penia peak (Fig. 1). Finally, the West Marmolada glacier (ID CGI 942) forms on the lower-most and western-most sector. Even though the possible presence of cold ice at the highest elevations cannot be ruled out a priori, the Marmolada is considered to be a temperate glacier.

The analyzed data set was recorded using a Hera-G system manufactured by Radar Systemtechnik—RST, and all the GPR profiles were originally interconnected, meaning that the data were acquired continuously while flying above the glacier and its surroundings. This allows us to evaluate different acquisition issues like data coherency at several crossing points, turnaround effects, data variations caused by changes in the flight elevation, and lateral effects above different portions of the glacier having quite different and paradigmatic characteristics (Fig. 1).

The equipment consists in a stepped-frequency radar (SFR), which uses a series of frequency bands combined in order to achieve the desired bandwidth. As opposed to impulse GPR, SFR systems typically transmit each frequency for a relatively long period of time, and the backward reflections are recorded while the transmitter is still emitting. From the amplitudes and phases sampled at each transmitted frequency, a synthetic spectrum is reconstructed and then transformed into a time series by applying the Inverse Fourier Transform. In general, the dynamic range achievable by SFR systems is limited due to the simultaneous operations of transmitting and receiving. In fact, strong signals coming from direct antenna coupling and surface reflections limit the overall sensitivity for weaker late signals. A possible strategy to partially overcome such limitations is gating. The Hera-G radar transmits narrow-frequency components in short pulses, while the receiving antenna is activated only when the transmitter is off. By choosing an appropriate time window for the receiver, the strong signals can be suppressed and a higher instrumental sensitivity can thus be reached. Additional technical details about the Hera-G system

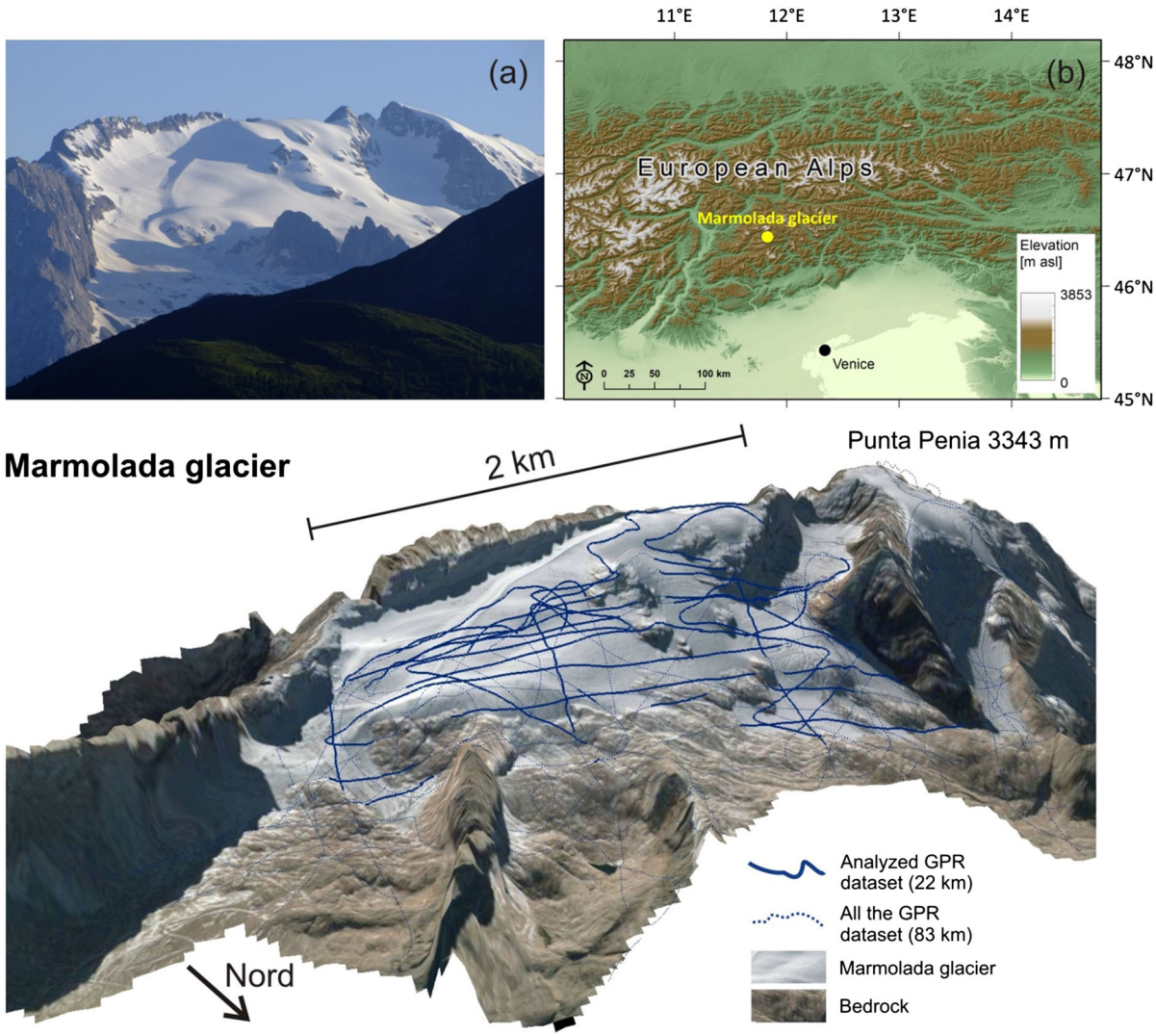

Figure 1
Location map of the Marmolada glacier, showing **a** the glacier as seen from Passo Falzarego, about 15 km to the north (photo taken by R.R. Colucci on July 8th 2014), and **b** the position of the glacier in the European Alps. The lower image shows the GPR acquisition paths superimposed to a 3D reconstruction of the Marmolada massif, realized by projecting a free image taken from Bing Maps on the high resolution Digital Elevation Model obtained from a 1 m cell LiDAR acquired in October 2014 by Helica srl

are provided by Krellmann and Triltzsch (2012), while further details about SFR operating principles can be found in Hamran et al. (1995).

The equipment used during the GPR survey, which includes the central unit, the antennas, and the GPS system, was mounted on a frame and suspended 10 m below an Eurocopter AS350 by cables connected to the cargo hook. The Hera-G system has a nominal central frequency equal to 100 MHz, however the amplitude spectrum obtained from the entire GPR data set shows an actual central frequency equal to 85 MHz (being the peak frequency equal to 66 MHz), and a quite large bandwidth with a homogeneous distribution (Fig. 2). The acquisition time window was set equal to 2225.09 ns and the signal was recorded with a 1.087 ns sampling interval, corresponding to a Nyquist frequency equal to

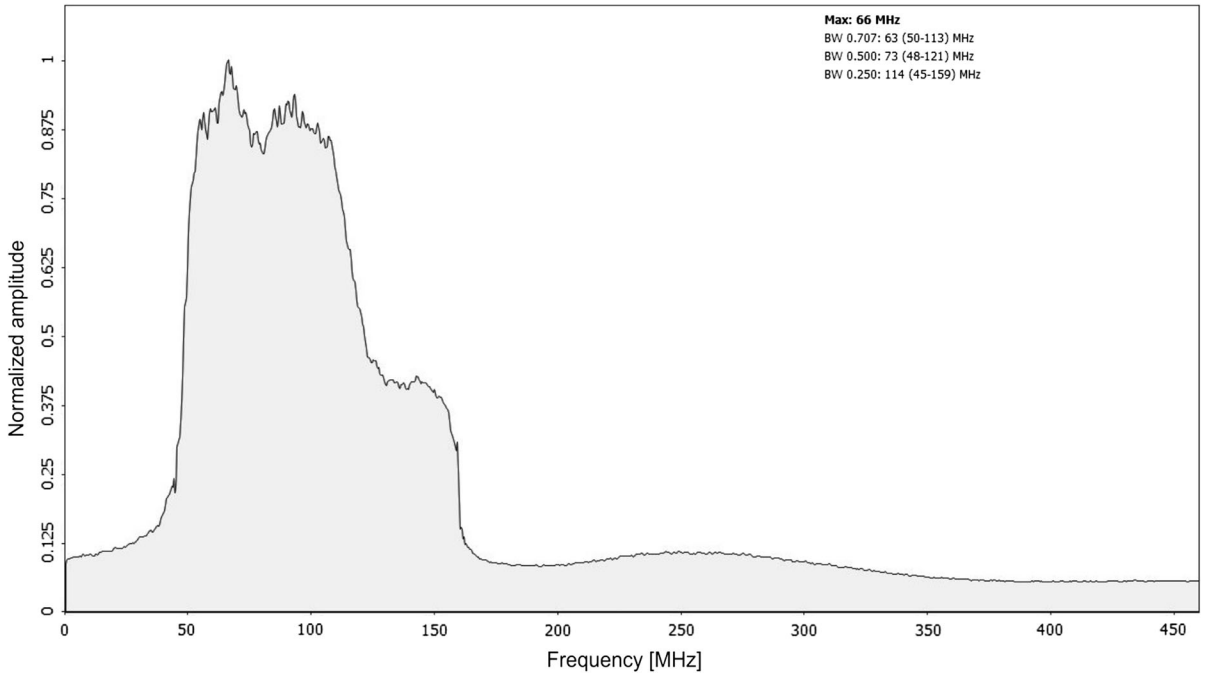

Figure 2
Normalized amplitude spectrum constructed from the entire GPR data set acquired on the Marmolada glacier (Fig. 1). The signal spectrum has a quite large bandwidth, with a quasi-homogeneous distribution and a central frequency equal to 85 MHz

Table 1
Synthesis of the parameters used in the applied processing flow

Processing flow	Parameters
Band-pass filter (Ormsby)	30–50–170–270 MHz
Datuming	Zero time at 3300 m a.s.l.
Elevation (static) correction	Values based on the helicopter radar altimeter
Exponential amplitude recovery	0.2 dB m

460 MHz, which is far higher than the highest useful signal frequency, equal to about 160 MHz (Fig. 2).

We applied a basic processing flow encompassing: band-pass filtering, datuming, topographic (static) corrections considering the variable flight elevation above the ground for each trace, and exponential amplitude recovery. All the data shown (except the one in Fig. 5b) are not migrated in order to make more apparent the effects of scattering on the data. However, we would like to remark that in general, in all GPR surveys, interpretation must be based on migrated sections (or volumes), which is something unfortunately not always done at present. Un-migrated data can be used for comparison because the un-migrated diffraction hyperbolas make the scatterers more apparent. In Table 1 we summarize the applied processing algorithms with the adopted parameters. The amplitude recovery considers a constant attenuation equal to 0.2 dB/m, which is higher than pure ice and qualitatively takes also into account for free water and scattering within the frozen materials.

3. *Analysis of Typical Issues for Helicopter-Borne GPR Surveys*

3.1. *Acquisition Paths, Antenna Orientation, and Possible Directional Dependency*

During airborne data acquisition in rugged mountainous regions, it is almost impossible to follow regular flight paths, mainly due to severe

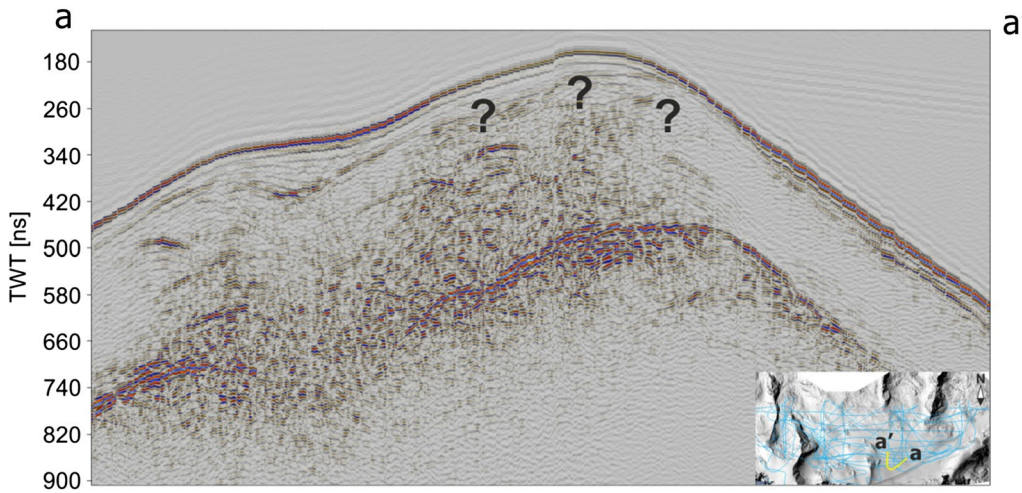

Figure 3
Example of a curvilinear GPR profile. The question marks highlight an area in which the lateral continuity of reflectors is very poor, due to the sharp curvature of the data acquisition path. Labels a-a' (as well as b-b', c–c',…) here and in Figs. 4, 7, 8 and 9 mark the lateral limits of the shown GPR profiles on the location map

topographical constraints and changing local atmospheric conditions. Moreover, the shape of reflecting surfaces, such as the interfaces between different frozen materials as well as the top of the bedrock, is intrinsically irregular, thus rendering unrealistic any effort to optimize the survey direction with respect to "planar" targets. In the central part of the GPR profile shown in Fig. 3, where the curvature of the flight path is higher, it is almost impossible to clearly image the reflector representing the firn-ice interface (i.e. question marks in Fig. 3).

In terms of target detectability, it is well known that for linearly elongated structures (like crevasses in glaciological surveys) the best results are obtained when the survey direction is almost perpendicular to the main axes of the targets. For example, Fig. 4 shows that crevasses, which are typically elongated structures within the glacier, can be better imaged when the GPR profiles are crossing them perpendicularly. A comprehensive mathematical review of this topic, which is outside the scope of this paper, can be found for instance in Dell'Acqua et al. (2004).

With regards to the antenna orientation, Rutishauser et al. (2016) pointed out that there is a possible decrease in the reflected amplitudes when the antennas are parallel to the survey direction. Similarly, Nobes (1999) observed that the detection of the basal reflection within glaciers is improved when using a parallel antenna orientation as opposed to a perpendicular one. Moran et al. (2003) also analyzed bedrock reflections for different antenna orientations on temperate glaciers, concluding that different antenna orientations can produce a remarkable reduction in the reflection amplitude. Two recent papers (Langhammer et al. 2017 and 2018) further investigate the effects due to antenna orientation, highlighting that directionality effects of the radiation pattern can significantly degrade the quality of the subsurface imaging when the GPR antennas are unfavorably orientated. As a possible solution, such Authors suggest using dipole antennas orientated parallel to the glacier flow direction for glaciers confined within a valley. When the general shape of the bedrock topography is unknown, a dual-polarization survey with a subsequent combination of data from both antenna polarizations is preferable.

It's interesting to remark that due to the above described GPR antenna orientation effects, which are in turn related to the radiation patterns of the used antennas, airborne GPR surveys are quite different from the ones involving other geophysical techniques like helicopter EM surveys, using both frequency- or time-domain instruments (FDEM and TDEM, respectively).

Figure 5 provides a comparison between unmigrated and migrated data. Migration was

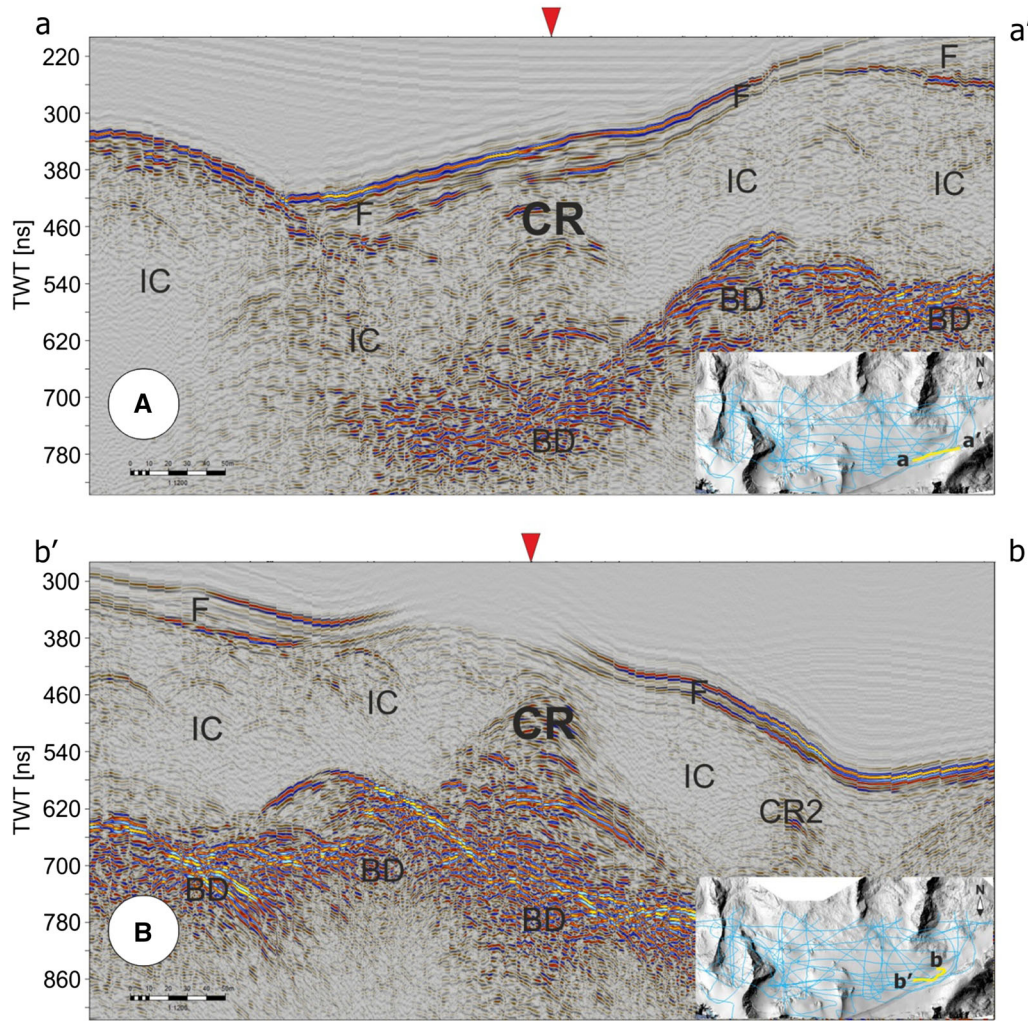

Figure 4
Example of two GPR profiles crossing each other (red triangle) directly above a crevasse (CR). The profile in (**B**) is almost perpendicular to the crevasse and therefore such structure is better imaged in (**B**) than in (**A**), where the profile crosses with the crevasse at a smaller angle. The labels highlight the main materials and structures within the glacier, including firn (F); ice (IC), bedrock (BD), and a secondary crevasse (CR2)

performed by applying a 2D Kirchhoff algorithm, with a simple EM velocity field characterized by a constant velocity for both firn (equal to 21.2 cm/ns, obtained by means of diffraction hyperbolas analysis and direct density data of a snow pit) and ice (equal to 17.0 cm/ns and inferred just by fitting of diffractions). While the imaging is overall acceptable and it is helpful to better define the geometry of the same crevasse (CR) shown in Fig. 4, as well as to focus some localized diffraction (d) most probably related to single blocks within the ice, some other wider diffractions (D) are not fully focused. The migration of airborne data acquired on rugged terrains and in presence of strong scattering would probably need a more sophisticated approach, which is out of the scope of this paper.

3.2. *Positioning Errors Caused by Oscillating Antennas*

When the GPR antennas are suspended below the helicopter, peculiar situations can arise (Fig. 6) due

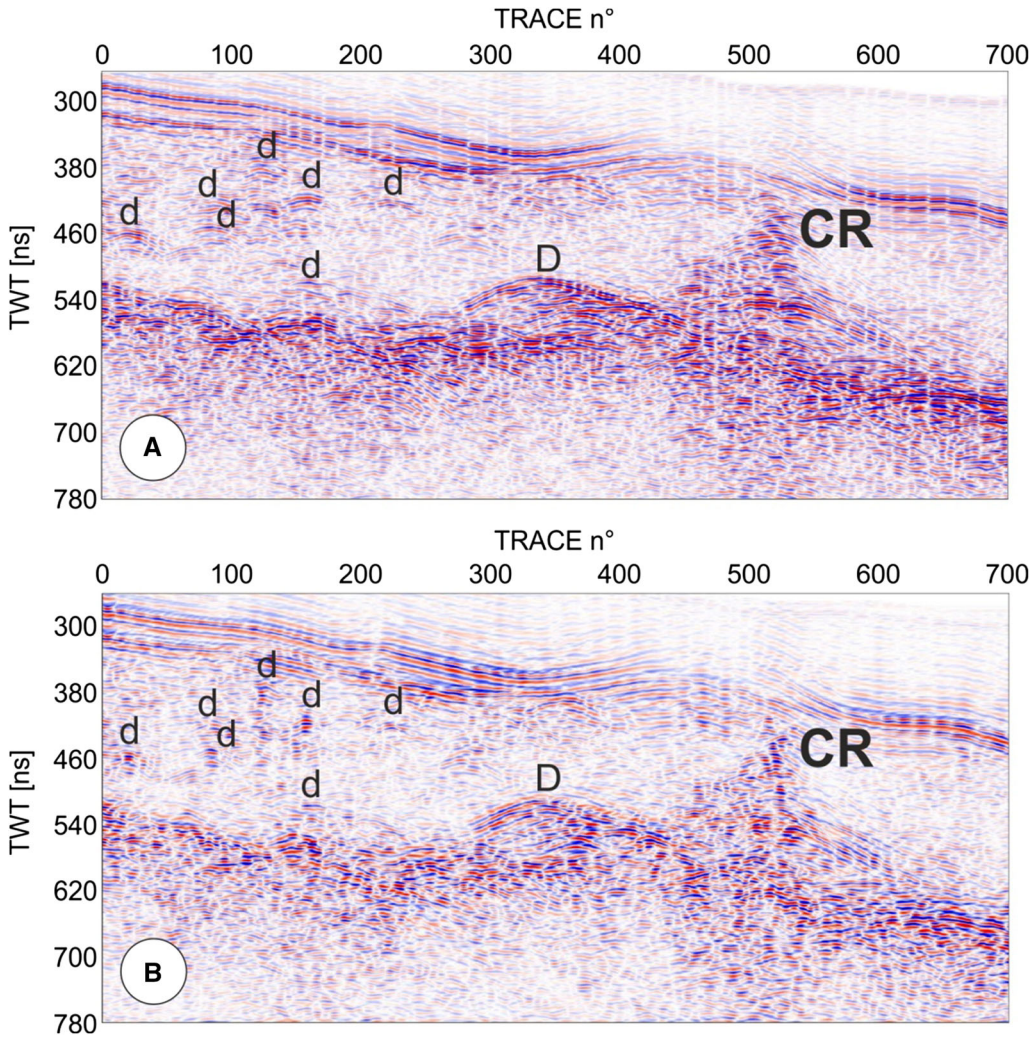

Figure 5
Example of comparison between un-migrated (**A**) vs. time-migrated data (**B**) performed on a portion of the same data shown in Fig. 4B. The figure shows several features, including a crevasse (CR), localized scatterers (d), and a wide diffraction (D). See text for further details

to the transational and rotational movements of the antennas introducing positioning errors both in the latitude (Δx), longitude (Δy), and altitude (Δz). It is almost impossible to quantify such errors, since they continuously change along the acquisition path, and they tend to increase when the GPS system is located on the helicopter rather than on the suspended antennas. It is also apparent from Fig. 6 that trace positioning errors tend to increase at higher elevations of the helicopter above the ground. In fact, given a certain antenna orientation, the shift between the recorded antenna position and the glacier section actually illuminated by the GPR signals increases with the elevation, thus further complicating the imaging of the internal glacier structures.

Mounting the antennas directly below the helicopter does not completely solve the problem, since possible trace positioning errors can still be introduced every time the helicopter turns or changes its altitude. Nevertheless, trace positioning errors can be minimized by acquiring straight profiles and by mantaining a constant or slowly changing flight speed, so that the antenna oscillations can be reduced, as well as the deviations of the illuminated point from

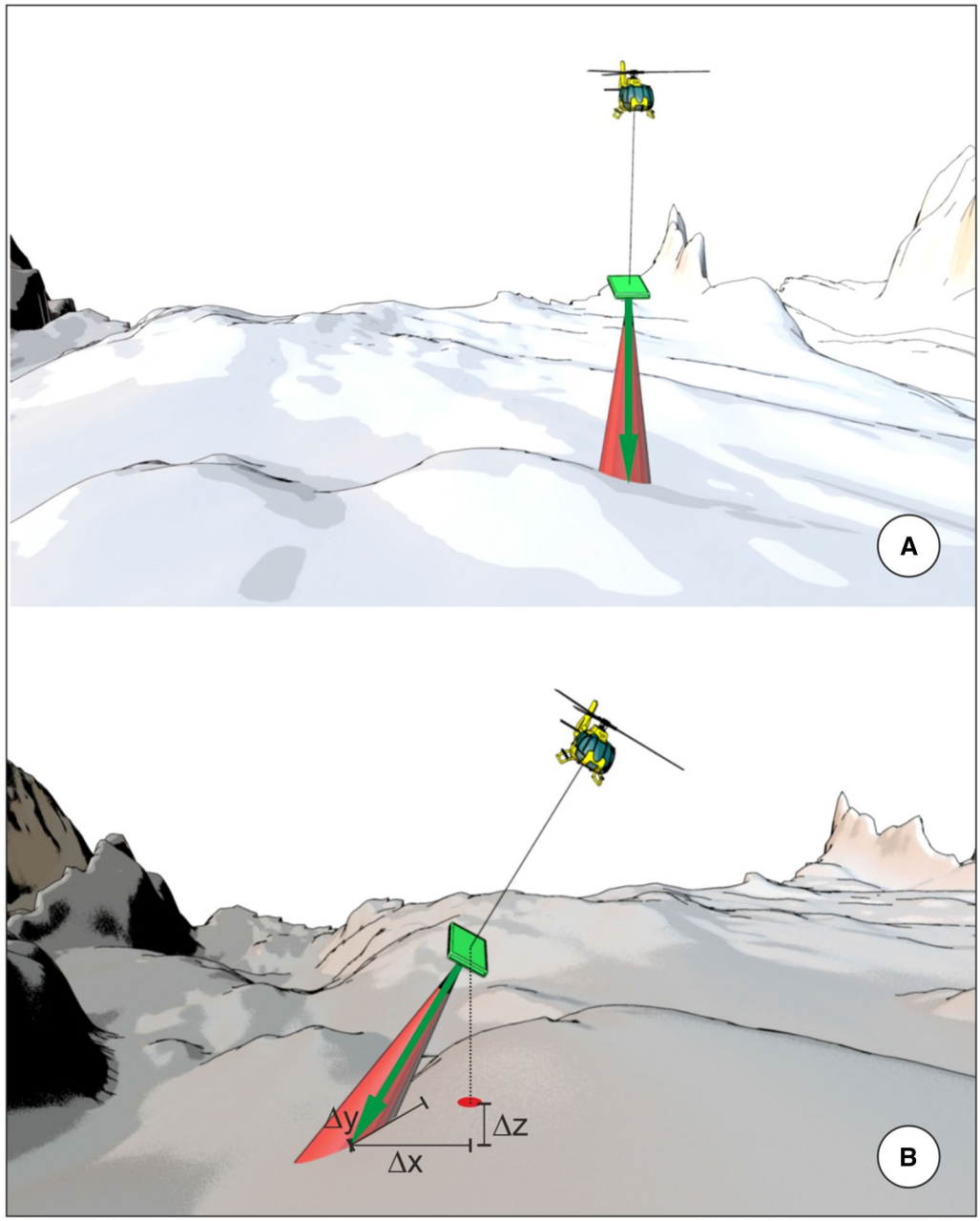

Figure 6
Example of possible trace positioning errors caused by the antenna oscillations, when hanging below the helicopter. When the antennas are located exactly below the aircraft there are no positioning errors (**A**), however possible deviations from the vertical position can introduce significant errors in the recorded latitude (Δx), longitude (Δy), and altitude (Δz) of the GPR profile, with respect to the actual illuminated area of the glacier (**B**)

the vertical. The positioning accuracy could also be increased by installing specific devices on the antennas like integrated GPS, eccelerometers and inclinometers, designed to measure at an adequate rate (e.g. around every second) the yaw, pitch and roll of the antenna. In this way, appropriate data

processing could be easily performed in order to calculate and correct for the antenna rotation and tilting. From a technical point of view, this would be a quite straighworward implementation of procedures originally developed for Autonomous Underwater Vehicles (AUV) and currently used in marine geophysics (Wynn et al. 2014). However, we remark that even by introducing such corrections and following a straight acquisition line, the resulting data would still not be actually along 2D straigth profiles due to the movements of the antenna producing a shifting of the illuminated area.

3.3. Positioning Errors Due to GPS

It is well known that any GPS device can have performance issues when working in mountain regions, especially when the GPS antenna operates in narrow valleys or near the mountain sides. In addition to a significant decrease in the accuracy of specific recorded trace positions, rapid and anomalous changes in the trace coordinates can occur when the satellite constellation abruptly changes. An example of this effect on GPR data is shown in Fig. 7a, where blue triangles mark clear and abrupt elevation shifts along the recorded profile. In such conditions, the data can only be corrected when different portions of the GPR profile show sensibly different values of the GPS data quality parameters (e.g. GDOP), or when independent data are available. In the latter case, the elevation measurements derived from GPS data can be verified and possibly corrected using Digital Elevation Models (DEM) derived from Light Detection and Ranging (LIDAR) or photogrammetric data. In fact, it is well known that the accuracy of GPS data is usually sensibly higher for the latitude and longitude coordinates, rather than the elevation. Surely specific GPS acquisitions can be exploited, including GPS able to receive signals even from GLONASS satellites to increase the chances of enough satellites for a more precise solution or dual-frequency receivers with either a local base station or a Precise Point Positioning service to post-process the data. Nowadays, in several parts of the world, there are base-station data available for free and/or real time GPS corrections (network real time kinematic—NRTK). However, in remote mountainous areas (like for instance in most of the Alps) the density of base stations is usually very low and the closest one can be several tens of km away from the survey area. Moreover, in some zones it is impossible to keep the signal for real-time corrections due to the absence or to a limited mobile phone signal availability. In any case, all the previously described strategies are more expensive, time consuming, and sometimes logistically difficult.

In Fig. 7b a GPR profile seemingly without any positioning error is shown, while in Fig. 7c the same profile is compared with two other intersecting profiles at their respective crossing points, marked by red triangles. In the latter example, while at point "c" the elevation of the two crossing profiles is almost identical, this is not the case at point "d" (Fig. 7c).

3.4. Topography-Related Issues

Peculiar artifacts can appear within airborne GPR data sets when flying too close to lateral structures (e.g. a rocky wall), such as the apparent doubling of the topographic surface, as well as of reflections and diffractions. This is due to lateral signals being erroneously imaged as if they originated along the flight path (Fig. 8). Since 2D migration algorithms applied during data processing offer only partial and limited solutions for out-off-plane events, the only effective strategy is to avoid flying along pathways characterized by strong lateral reflectors. Given the typical geometry of cirque glaciers, it is advisable to collect data following the maximum surface dip, while trying to avoid when possible paths along constant topographic elevations so that higher terrains do not become possible lateral reflectors. Sometimes lateral signal can be easily detected and separated from the actual information (Fig. 8a), however there are many cases in which signal interference prevents any reasonable data interpretation (Fig. 8b). Specific imaging strategies can be adopted in order to minimize the artifacts, while improving the accuracy in the subsurface geometry reconstruction (Lehmann and Green 2000; Bradford et al. 2015), but in order to do that some parameters, like the EM velocity field, must be known with a very high accuracy level.

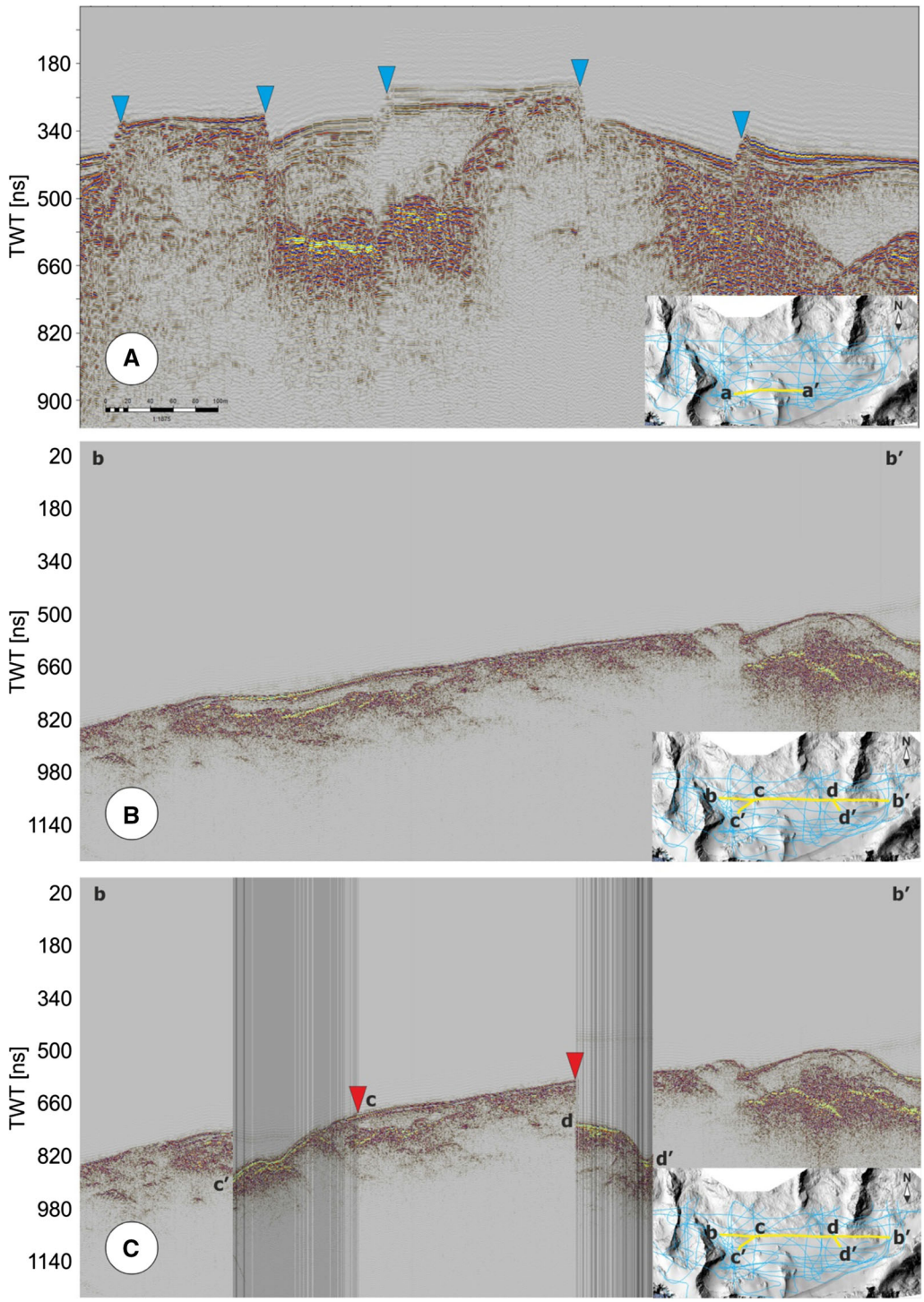

Figure 7
Example of possible issues related to the GPS positioning. The figure shows **A** a GPR profile affected by several abrupt elevations shifts (blue triangles); **B** a profile without any apparent positioning error; and **C** the same profile in (**B**) compared with two intersecting profiles at the respective crossing points (red triangles). While the intersection with profile c–c′ is almost perfect, this is not the case for the intersection with profile d–d′

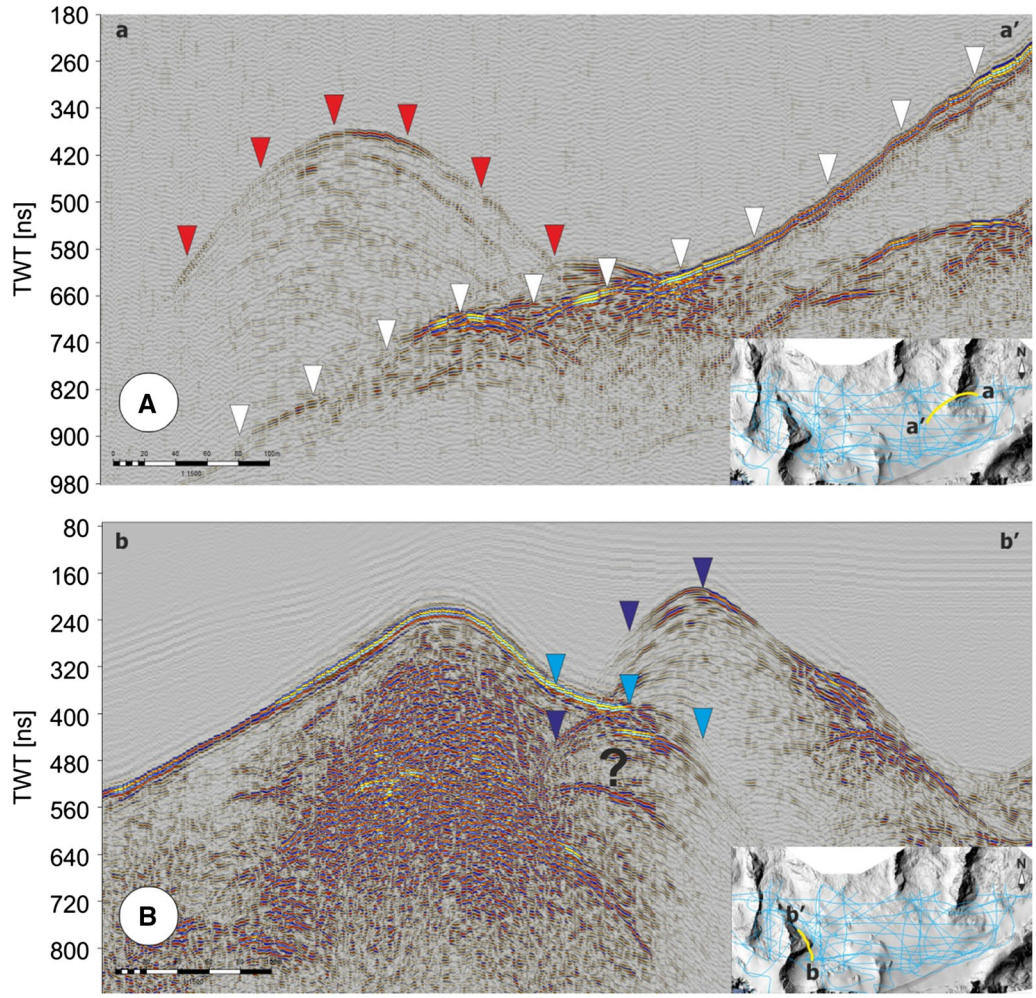

Figure 8
Examples of detection of reflected and diffracted signals originating from lateral structures: **A** the red triangles mark the top of a lateral signal, while the white triangles mark the actual topography, which is still recognizable; **B** the light and dark blue triangles mark superimposed signals coming from lateral interfering events, which cannot be separated. The question mark in (**B**) highlights a zone which cannot be accurately interpreted

3.5. Effects of the Flight Elevation Above the Ground

As previously discussed, the amplitudes of the recorded GPR signals tend to decrease with the increasing antenna elevation above the ground, due to higher spreading losses caused by wavefront expansion. This effect has been studied for airborne GPR systems by collecting data during the helicopter take-off (Altdorff et al. 2014), as well as for commercial GPR systems by analyzing total reflections from a metallic surface (Dossi et al. 2018). Both these approaches observe an asymptotic 1/r amplitude decay with distance caused by wavefront expansion, which is consistent with the theoretical GPR antenna radiation models. In particular, for air-coupled GPR antennas, the signal wavefronts propagating in air can be approximated with an expanding hemisphere, with the data showing similar amplitude decays independently from the antenna orientation (Dossi et al. 2018). Therefore, in order to reduce the distance traveled by the recorded signals, it would be preferable to fly as close as possible to the topographic surface during any airborne survey, obviously taking

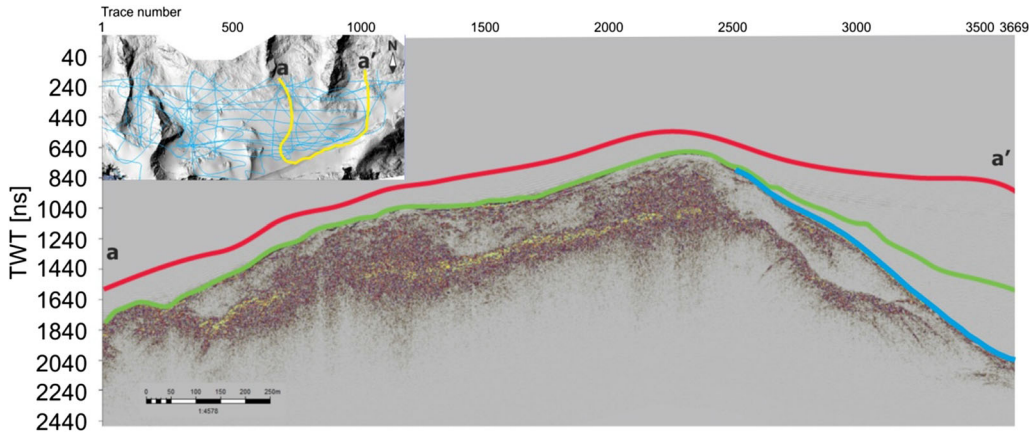

Figure 9
Exemple of an airborne GPR profile acquired with laterally variable antenna elevation above the surface. The flight elevation (red line) above the topographic surface does not change considerably in the 1–2500 trace interval, while it rapidly increases after trace 2500. The time-position of the surface reflection (blue line) along the GPR profile significantly differ in the 2500–3669 trace interval from the actual topography (green line), obtained from independent LiDAR data

all the safety precautions and considering all the logistical constraints.

Amplitude recovery can theoretically be used to compensate for the spreading losses caused by increasing elevation, however it is important to point out that the processed data would still be affected by a lower signal-to-noise (S/N) ratio. More importantly, Fig. 9 shows that peculiar effects can occur when the flight elevation above the topographic surface changes during data acquisition. Specifically, when the antenna elevation is high (e.g. right side in Fig. 9) the position of the surface reflection in the GPR profile can significantly differ from the measured elevation of the recorded traces. This effect produces noticeable discrepancies between the actual topography (green line in Fig. 9), extrapolated from independent LiDAR data, and the apparent one (blue line) observed in the GPR profile. These discrepancies are quite unpredictable and difficult to correct even with sophisticated migration algorithms; therefore we suggest keeping a constant elevation above the surface, when possible. In addition, it would be advisable to collect several intersecting GPR profiles, since each intersection represents a control point at which the data can be cross-checked and validated (Fig. 10). Surely, the details of imaging at the crossing points can be slightly different due to the different reflection pattern reaching the target (Langhammer et al. 2018) but the depth of the main reflectors should be consistent.

3.6. Flight Speed Issues

It is well known that the lateral resolution within a GPR profile is inversely proportional to the radius of the first Fresnel zone (R_f), which is approximated by the following equation:

$$R_f \cong \sqrt{dv/2f} \tag{2}$$

where d is the distance of the target from the transmitter, v is the average EM velocity above the target, and f is the frequency of the EM signal. This formula is strictly valid only for monochromatic signals and for unfocused waves, and since all the commercial impulsive or step frequency GPR systems employ ultra-wide band wavelets and directive antennas, the accuracy of the Fresnel criterion (Eq. 2) is limited to just the order of magnitude. In addition, the lateral resolution of any GPR survey is diminished when the trace interval increases. For specific helicopter-borne surveys, Gusmeroli et al. (2014) report good quality data collected with a flight speed of about 20 $m \cdot s^{-1}$ (i.e. about 40 Kt), while Machguth et al. (2006) suggest optimal data acquisition velocities close to 5 $m \cdot s^{-1}$ (i.e. about 10 Kt). In our experience, it is almost impossible and actually meaningless to

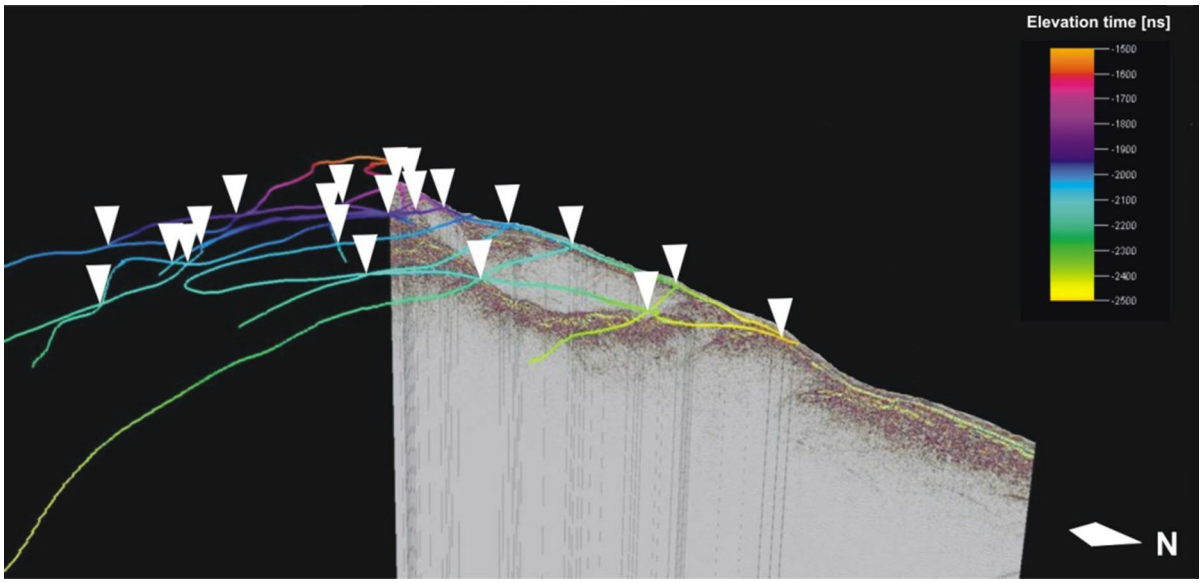

Figure 10
Example of validation of the interpreted results at each crossing point (white triangles) between different GPR profiles

suggest either a maximum trace interval or a maximum flight speed, because both parameters strictly depend on the objectives of the survey, the acquisition parameters, and the local topography. For instance, in order to obtain a detailed mapping of the snow cover on a smooth topography, the minimum acquisition rate can be in the order of 0.5 traces·m^{-1} (Gusmeroli et al. 2014), however the acquisition rate must be equal to at least 0.2 traces·m^{-1} in order to accurately image the firn-ice and ice-bedrock interfaces. Similar surveys performed over relatively coarse non-glacial terrains were unsuccessful, as reported for instance by Gusmeroli et al. (2014).

An example of lateral resolution analysis is given in Fig. 11, where the same portion of a GPR profile is plotted using trace intervals respectively equal to 1.6 (A), 3.2 (B), 6.4 (C) and 12.8 (D) m. The figure shows that while trace intervals up to about 3 m long are small enough to detect both the firn-ice and the ice-bedrock interfaces, preserve the shape of diffraction hyperbolas, and consequently allow their fitting for EM velocity analysis (see e.g. Forte and Pipan 2017), the data quality is rapidly diminished at larger intervals. It is also quite apparent from Fig. 11c and d that the deepest parts of both the aforementioned reflectors are not affected by aliasing at those trace intervals, while the parts exhibiting an almost flat shape are still recognizable even with trace intervals up to about 10 m long. Since the maximum dip of the targets cannot usually be predicted before the geophysical survey, or at most it can be roughly estimated, a minimum trace interval should be considered in order to prevent spatial aliasing and possible information losses. In fact, while a horizon may be detected even with large trace intervals, the same data may not necessarily be useful to accurately estimate the depth of such horizon, or to highlight its morphological details.

Spatial aliasing problems are general and can affect any GPR survey, however helicopter-borne data can suffer possible additional issues related to the lateral resolution. In fact, the lateral resolution does not only depend on the size of the Fresnel's zone and on the trace interval, but also on the elevation of the antennas above the ground. A trade-off between all these parameters has to be considered, especially when the antenna elevation increases. Figure 12 qualitatively shows that while the elevation has a marginal effect for relatively flat topographies (A), in the presence of a rough surface, lateral effects are more prominent at higher elevations (e.g. H in Fig. 12b), while the lateral resolution is reduced

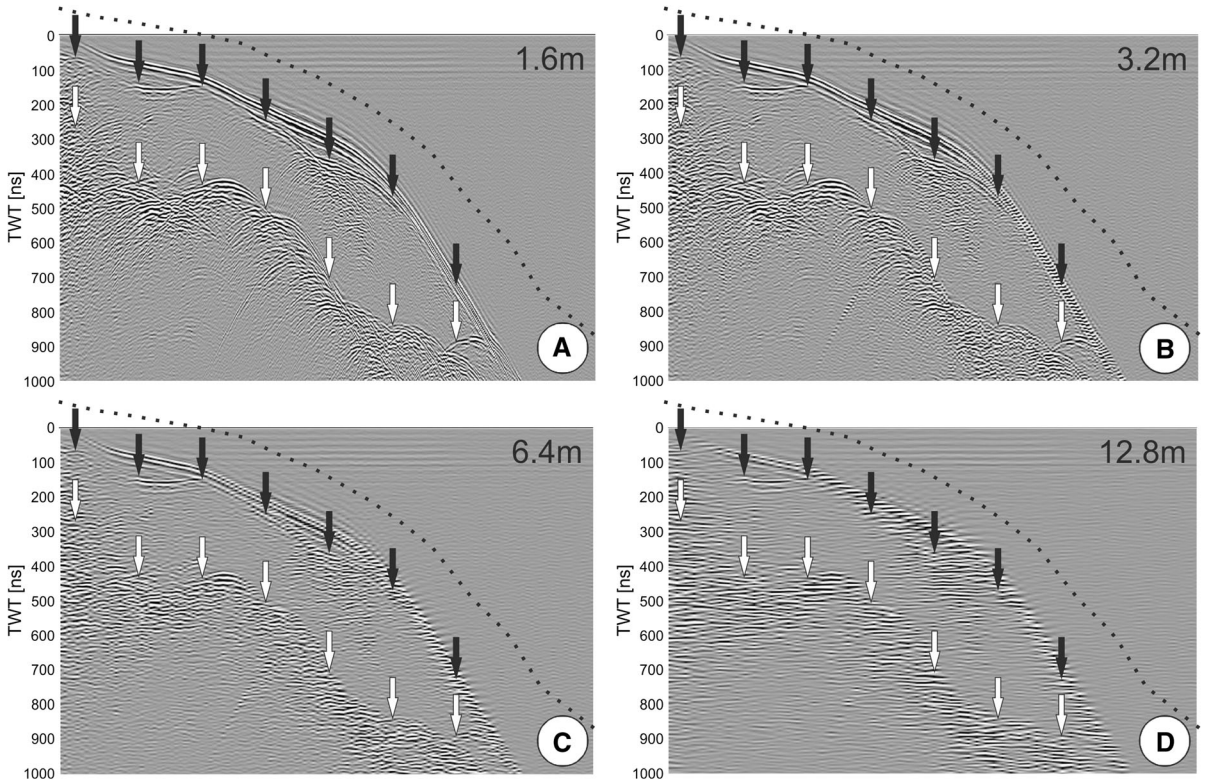

Figure 11
Example of spatial aliasing effects along the same airborne GPR profile for different trace intervals. The original profile has a 1.6 m trace interval (**A**), subsequently increased to 3.2 m (i.e. 1 trace every 2) in (**B**); 6.4 m (i.e. 1 trace every 4) in (**C**); and 12.8 m (i.e. 1 trace every 8) in (**D**). The dotted line indicates the time-position of the antennas above the topographic surface, plotted considering a constant EM velocity equal to 30 cm/ns, while the different arrows mark the interpreted firn-ice (black arrows) and ice-bedrock (white arrows) interfaces

due to a larger footprint, and the data interpretation becomes more difficult. Figure 12 also shows similar results when less focused signals are used, since this latter case mimics a higher elevation of the antennas above the topographic surface (e.g. U in Fig. 12a). In general, when the antennas are far away from the ground surface, more signal is lost into the air and the performance of the GPR system is reduced. On the other hand, the main advantage of any air-coupled system is that the antenna coupling does not change along the GPR profile like it does in ground-based surveys due to the varying EM properties of the surface material (e.g. Annan et al. 1975).

The helicopter has the ability to fly with a wide speed range or even stopping in mid-air. This obviously represents a great advantage for many applications, but an inconstant data acquisition velocity can produce a variable trace interval when the triggering is at constant time intervals. This can in turn produce spatial aliasing and prevent the use of several processing algorithms (e.g. migration) which perform better with regular spatial sampling. Therefore, it could be worthwhile to reduce the trace interval in order to obtain a moderate spatial oversampling, which allows to eliminate surplus traces thus reconstructing almost equally spaced data sets. From the point of view of the helicopter, it is quite obvious that the pilot should keep the flight speed as constant as possible.

3.7. Helicopter Piloting Issues

Airborne geophysical surveys are very difficult to carry out over rough topography, especially when the survey instruments are towed below the helicopter as cargo. The skill and experience of the pilot are

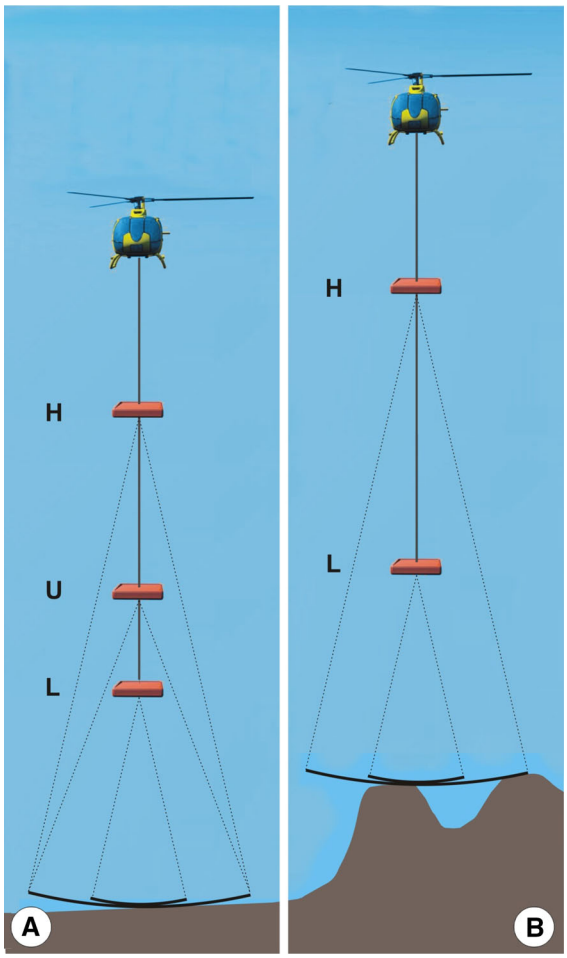

Figure 12
Illustration of the effects of the antenna elevation and signal focusing on the lateral resolution of GPR data sets acquired on both flat (**A**) and rough (**B**) terrains, for low (L) and high (H) antenna elevations above the ground. The letter U marks a peculiar case in which a less focused transmitter is used, producing results similar to the ones obtained at higher elevations (H)

undoubtedly the most important factors, however they are not the only ones and other objective evaluations must be taken into account. Detailed safety prescriptions about airborne geophysical surveys are provided by the International Airborne Geophysics Safety Association (IAGSA, http://www.iagsa.ca), which is a nonprofit international association whose mandate is to promote and enhance safety in the airborne geophysics survey industry. We remark that a pilot with a deep knowledge of the survey area, and with specific experience in geophysical data acquisition, is helpful in any survey, but it is mandatory in mountainous areas.

Since a rough terrain does not facilitate a regular flight pattern, it is preferable to acquire the data climbing the fall line of the mountain, and keeping the azimuth as constant as possible. In fact, for aeronautical reasons, the helicopter can easily fly up the mountains, however during descent the pilot must reduce the speed in order to keep a constant terrain clearance. This inevitably causes the towed instruments to become unstable, with the antennas turning on itself, resulting in completely staggered measurements. Therefore, the ideal flight path would contain lines that climb up the mountain (red lines in Fig. 13), with the helicopter flying at an altitude defined by a pre-planned drape surface, taking into account the DEM and a constant terrain clearance. Moreover, such profiles would be almost perpendicular to the most common linearly elongated structures within the glacier (e.g. crevasses C in Fig. 13), thus improving their detection as previously discussed. In addition, it is possible to acquire zigzag profiles (green lines in Fig. 13) to allow data validation at each crossing point between profiles (Fig. 10), as well as other profiles at almost constant elevations over favorable areas (yellow lines in Fig. 13).

4. Discussion and Guidelines

In the previous sections, we highlighted several peculiar issues arising from helicopter-borne surveys performed in mountain regions. Specifically, we highlighted pros and cons of the data acquisition method by analyzing an airborne GPR data set acquired on the Marmolada glacier (Fig. 1). From our analysis, we provide some general guidelines and possible optimization strategies, summarizing in Table 2 the most common issues. The topics listed in the table can be grouped into three conceptually distinct categories of airborne GPR acquisition problems, namely: (1) a variable geometry; (2) changing acquisition parameters; (3) malfunctioning instruments or inaccurate measurements.

1. Changing or inconstant geometry can arise when data acquisition paths are characterized by sharp curvatures, or when the antennas suspended below the helicopter oscillate. When the antennas are

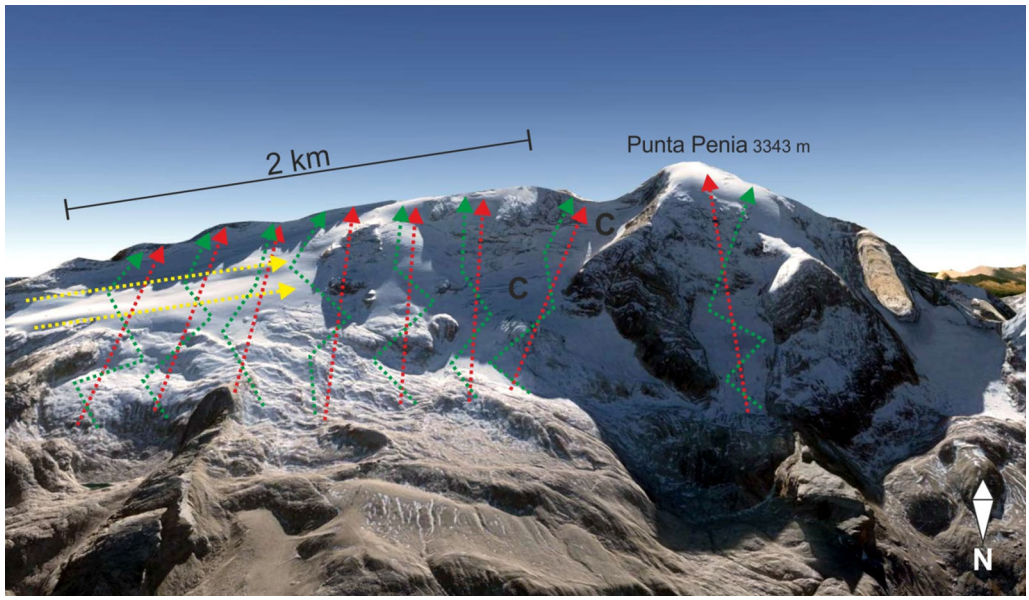

Figure 13
Example of ideal flight patterns superimposed on the Marmolada DEM. The figure shows straight paths along the maximum elevation gradients (red lines); possible zigzag complementary flight patterns (green lines), which can be used to verify the data coherency at each crossing points between GPR profiles; and possible additional profiles in areas with relatively smooth topography (yellow lines). The presence of crevasses is also highlighted (C)

mounted directly on the helicopter skids this problem is negligible, however, the disadvantage of this setup is an increased amount of ringing noise originating from the EM interferences between the antennas and the helicopter, which is not easy to remove and can mimic actual reflectors (Rutishauser et al. 2016). On the other hand, the main advantage of such configuration is that the antennas are truly oriented along the flight direction and their orientation remains constant, as opposed to any suspended device.

2. Variations in the data acquisition parameters are mainly caused by a changing flight speed, which produces an inconstant trace interval and can introduce spatial aliasing. In our analysis, we observed that a moderate spatial oversampling can solve most of the problems related to this issue, while redundant traces can be reduced afterward (trace decimation or binning) to obtain the desired constant trace interval. Modern GPR systems, both impulsive and SFR, allow fast data recording, thus preventing spatial sampling limitations, except in the case of very high-speed helicopter-borne surveys (Hamran et al. 1995). As previously discussed, additional problems are related to changes in the antenna elevation above the ground, which produce variations in the antenna footprint and possible reflections and diffractions from lateral structures as the elevation above the ground increases.
3. The GPR data can also be affected by trace positioning errors, which occur when the GPS antenna receives signals from a limited number of satellites, and when the geometry of the detected satellite constellation is asymmetric or changes abruptly over time. Malfunctions of the GPR device are rarer; however some instruments are not perfectly repetitive, therefore the recorded reflection amplitudes may also be affected by the unpredictable transmitted wavelet, in addition to the other external factors.

The processing flow of helicopter-borne GPR data sets is similar in principle to the one commonly used for ground-based surveys and it is not discussed in detail in this paper. However, the peculiar characteristics of airborne systems make the data migration more difficult, since it is almost impossible to exclude

Table 2

Analysis of the most common issues encountered when performing helicopter-borne GPR surveys on rugged mountainous areas, general guidelines, and optimization strategies

Issue	Occurrence	Significant effects on GPR data	Guidelines and optimization strategies
1. Limited horizon detectability due to curvilinear profiles	Frequent for relatively small survey areas with logistical constraints	Phase discontinuity Signal interference	Limit the maximum profile curvature Avoid rapid direction changes Acquire perpendicular profiles with respect to visible and regular linear targets
2. Oscillating antennas; variations in the antenna-ground angle	Typical for suspended antennas, and to some extent also when fixed on the helicopter	Trace positioning errors Lateral reflections and diffractions Inaccurate imaging of the subsurface	Limit the lenght of the suspension cables Avoid abrupt changes in the flight trajectory Avoid data acquisition in windy days Inserting additional positioning sensors on the antenna
3. GPS malfunctions	Random, especially in narrow valleys with limited satellite detection	Abrupt apparent topographic changes Mismatching at the crossing points between profiles	GPS data quality checks with possible thresholds/filters Integrating independent DEM to infer the correct topography along the acquisition paths
4. Changing lateral topography	Very common in mountain areas, especially in narrow valleys or cirques	Lateral reflections and diffractions Signal interference	Keep a minimum distance from rock faces Acquire data along the mountain fall line
5. Changes in the helicopter elevation above the ground	Common, especially on irregular topography	Changing size of the antenna footprint Inaccurate topography and subsurface imaging	Avoid abrupt elevation changes Keep a costant elevation from the ground when possible Acquire intersecting profiles to allow data validation at the crossing points
6. Flight speed variations	Random	Irregular trace interval Possible spatial aliasing Limited lateral resolution and target detection	Set a reference flight speed based on the survey targets Avoid rapid changes in the flight speed Moderate lateral oversampling to prevent spatial aliasing

out-off-plane diffractions, which would be focused by using a velocity higher than the real one, thus degrading the overall quality of the profiles due to unavoidable artifacts. Therefore, a 3D migration is mandatory, although it would certainly be challenging for data sets consisting of widely and irregularly spaced 2D GPR profiles. Furthermore, specific algorithms should be considered in order to attenuate ringing when the antennas are mounted directly on the helicopter skids.

5. Conclusions

We analyze possible issues related to helicopter-borne GPR data acquisition in rugged areas, which can affect the overall data quality and possibly prevent the extraction of either qualitative or quantitative information from the recorded data set. These issues can be addressed by optimizing the data acquisition procedures, which could limit the quantity of recorded data and also reduce the required acquisition and processing times. For example, of the original 83 km long data set, we were able to use only 22 km (i.e. 26.5% of the recorded data) to model the Marmolada Glacier, since all the other profiles were severely affected by many of previously discussed problems, like trace positioning errors, lateral signal interference, data interpretation issues, or overall low signal-to-noise ratio.

In glaciological surveys, it is not only important to accurately detect the ice-bedrock interface, but also to quantitatively characterize the frozen material within glaciers, as well as their internal layering and

debris content. For example, relatively thick snow and firn layers can exist above the actual ice mass, especially in cold environments where the snow metamorphism is slower than in temperate glaciers. In order to obtain an accurate glacier model, we need not only low frequency components able to reach the ice-bedrock interface, and possibly go even deeper, but also high frequencies able to guarantee a sufficient vertical resolution so that the internal layering and main EM impedance contrasts can be detected. For any quantitative analysis or inversion, all spectral components must be properly recorded, while amplitude or phase distortions related to data acquisition procedures or signal processing must be limited as much as possible. In fact, quantitative GPR analyses are becoming more and more important (Gundelach et al. 2010; Gacitua et al. 2015; Dossi et al. 2016), trying to combine the subsurface imaging with a detailed quantification of physical parameters like EM velocity, free water content, and ice temperature. The general guidelines and optimization strategies provided in this paper can be helpful to address these topics and are still valid for UAV mounted GPR, which will probably become more common in the near future. Further research could address the quantitative analysis of airborne GPR data sets, exploiting their independence from the antenna-ground coupling as opposed to ground-based systems. As far as processing issues, a deeper investigation on imaging in such complex wave propagation conditions characterized by high scattering, as well as vertically and laterally inhomogeneous velocity could be an additional field of study.

Acknowledgements

This research is partially founded by the "Progetti di Ricerca di Rilevante Interesse Nazionale-PRIN 2015", Grant number 2015N8F555. We thank the management of Helica srl (Amaro, Italy) for the permission to use and publish the airborne GPR data set, and we gratefully acknowledge Schlumberger through the University of Trieste Petrel® interpretation package academic grant. We also thank ARPAV, in particular Anselmo Cagnati, Valter Cagnati, and Andrea Crepaz, as well as Costanza Dal Gobbo for her help in the survey planning, and Manja Žebre and Daniele Fontana for assisting in the field operations. Authors are also thankful to Dr. Pierre Keating, Associate Editor, and two anonymous reviewers for providing thoughtful and useful comments and suggestions.

Author contributions EF and RRC conceived the work; MBB analyzed the GPR data set and prepared some figures; EF wrote the paper with contributions from AB (piloting issues), MD (GPR) and RRC (survey area), and edited all the figures. All the authors revised the final version of the manuscript.

Publisher's Note Springer Nature remains neutral with regard to jurisdictional claims in published maps and institutional affiliations.

References

Altdorff, D., Schliffke, N., Riedel, M., Schmidt, V., van der Kruk, J., Stoll, J. B., & Becken, M. (2014). *UAV borne electromagnetic induction and ground-penetrating radar measurements: a feasibility test*. In 74th Annual Meeting of the Deutsche Geophysikalische Gesellschaft in Karlsruhe, Germany, March 9–13, 2014.

Annan, A. P., Waller, W. M., Strangway, D. W., Rossiter, J. R., Redman, J. D., & Watts, R. D. (1975). The electromagnetic response of a low-loss, 2-layer, dielectric earth for horizontal electric dipole excitation. *Geophysics, 40*(2), 285–298.

Arcone, S. A. (2002). Airborne-radar stratigraphy and electrical structure of temperate firn: Bagley ice field, Alaska, USA. *Journal of Glaciology, 48*(161), 317–334.

Arcone, S. A., Lawson, D. E., & Delaney, A. J. (1995). Short-pulse radar wavelet recovery and resolution of dielectric contrasts within englacial and basal ice of Matanuska Glacier, Alaska, USA. *Journal of Glaciology, 41*(137), 68–86.

Bahr, D. B., & Radić, V. (2012). Significant contribution to total mass from very small glaciers. *The Cryosphere, 6,* 763–770.

Birken, R., & Versteeg, R. (2000). Use of four-dimensional ground penetrating radar and advanced visualization methods to determine subsurface fluid migration. *Journal of Applied Geophysics, 43,* 215–226.

Blindow, N., Salat, C., Gundelach, V., Buschmann, U., & Kahnt, W. (2011). Performance and calibration of the helicopter GPR system BGR-P30. In *6th International workshop on advanced ground penetrating radar (IWAGPR)*, 22–24 June 2011, Aachen, Germany, pp 5.

Bradford, J. H. (2015). Reverse-time prestack depth migration of GPR data from topography for amplitude reconstruction in complex environments. *Journal of Earth Science, 26*(6), 791–798.

Bradford, J. H., Dickins, D. F., & Brandvik, P. J. (2010). Assessing the potential to detect oil spills in and under snow using airborne

ground-penetrating radar. *Geophysics, 75*(2), G1–G12. https://doi.org/10.1190/1.3312184.

Bradford, J. H., Harper, J. T., & Brown, J. (2009). Complex dielectric permittivity measurements from ground-penetrating radar data to measure liquid water content in snow in the pendular regime. *Water Resources Research, 45*(8), W08403.

Cabrera, R. A., & Bekic, G. (2018). Drone-borne ground-penetrating radar suitability for specific surveys: a comparative study of feature sizes versus antenna frequency and elevation over the ground. *First Break, 36*(8), 83–89.

Catapano, I., Crocco, L., Krellmann, Y., Triltzsch, G., & Soldovieri, F. (2012). A tomographic approach for helicopter-borne ground penetrating radar imaging. *Geoscience and Remote Sensing Letters, IEEE, 9*(3), 378–382.

CGI—Comitato Glaciologico Italiano (1978–2010). Relazioni delle campagne glaciologiche—reports of the glaciological surveys. *Geografia Fisica e Dinamica Quaternaria*, pp 1–34. (http://www.glaciologia.it/en/i-ghiacciai-italiani/le-campagne-glaciologiche/).

Conyers, L. B. (2013). *Ground-penetrating radar for archaeology* (3rd ed., pp. 258). Lanham: AltaMira Press.

Cook, J. C. (1960). Proposed monocycle pulse VHF radar for airborne ice and snow measurement. *Transactions of the American Institute of Electrical Engineers Part I (Communications and Electronics), 79,* 588–594.

Crepaz, A., Cagnati, A., & De Luca, G. (2010). Evoluzione dei ghiacciai delle Dolomiti negli ultimi cento anni e recenti bilanci di massa in tre apparati glaciali. *Aineva Journal, 4,* 20–25. **(in Italian)**.

Daniels, D. (2004). *Ground penetrating radar*. *IEE*, 2nd Ed. (pp. 752). London, UK: The Institution of Electrical Engineers.

Dell'Acqua, A., Sarti, A., Tubaro, S., & Zanzi, L. (2004). Detection of linear objects in GPR data. *Signal Processing, 84,* 785–799.

Dossi, M., Forte, E., & Pipan, M. (2018). Quantitative analysis of GPR signals: transmitted wavelet, amplitude decay, and sampling-related amplitude distortions. *Pure and Applied Geophysics, 175*(3), 1103–1122. https://doi.org/10.1007/s00024-017-1752-2.

Dossi, M., Forte, E., Pipan, M., Colucci, R. R., & Bortoletto, A. (2016). Automated reflection picking and inversion: Application to ground and airborne GPR surveys. In *Extended abstracts of the 16th international conference on ground penetrating radar (GPR2016)* (pp. 6). https://doi.org/10.1109/icgpr.2016.7572640.

Evans, S., & de Robin, G. Q. (1966). Glacier depth-sounding from the air. *Nature, 210,* 883–885. https://doi.org/10.1038/210883a0.

Fasano, C., Renga, A., Rodi Vetralla, A., Ludeno, G., Catapano, I., & Soldovieri, F. (2017). Proof of concept of micro-UAV-based radar imaging. In *International conference on unmanned aircraft systems (ICUAS)* (pp 1316–1323), June 13–16, 2017, Miami, FL, USA.

Forte, E., Dossi, M., Colle Fontana, M., & Colucci, R. R. (2014). 4-D quantitative GPR analyses to study the summer mass balance of a glacier: a case history. In *Proceedings of the 15th International Conference on Ground Penetrating Radar (pp. 352–356). GPR 2014*, 6970444.

Forte, E., Dossi, M., Colucci, R. R., & Pipan, M. (2013). A new fast methodology to estimate the density of frozen materials by means of common offset GPR data. *Journal of Applied Geophysics, 99,* 135–145. https://doi.org/10.1016/j.jappgeo.2013.08.013.

Forte, E., & Pipan, M. (2017). Review of multi offset GPR applications: data acquisition, processing and analysis. *Signal Processing, 132C,* 210–220. https://doi.org/10.1016/j.sigpro.2016.04.011.

Fu, L., Liu, S., Liu, L., & Lei, L. (2014). Development of an airborne ground penetrating radar system: antenna design, laboratory experiment, and numerical simulation. *IEEE Journal of Selected Topics in Applied Earth Observations and Remote Sensing, 7*(3), 761–766. https://doi.org/10.1109/JSTARS.2014.2303073.

Gabbi, J., Farinotti, D., Bauder, A., & Maurer, H. (2012). Ice volume distribution and implications on runoff projections in a glacierized catchment. *Hydrology and Earth System Sciences, 16,* 4543–4556. https://doi.org/10.5194/hess-16-4543-2012.

Gacitúa, G., Uribe, J., Wilson, R., Loriaux, T., Hernández, J., & Rivera, A. (2015). 50 MHz helicopter-borne radar data for determination of glacier thermal regime in the central Chilean Andes. *Annals of Glaciology, 56*(70), 193–201. https://doi.org/10.3189/2015AoG70A953.

Godio, A. (2009). Georadar measurements for the snow cover density. *American Journal of Applied Sciences, 6*(3), 414–423.

Gundelach, V., Blindow, N., Buschmann, U. (2010). Exploration of geological structures with GPR from helicopter and on the ground in the Letzlinger Heide (Germany). In *13th International Conference on Ground Penetrating Radar (GPR)* (pp. 6). 21–25 June 2010, Lecce, Italy.

Gusmeroli, A., Wolken, G. J., & Arendt, A. A. (2014). Helicopter-borne radar imaging of snow cover on and around glaciers in Alaska. *Annals of Glaciology, 55*(67), 78–88. https://doi.org/10.3189/2014AoG67A029.

Hamran, S. E., Gjessing, D. T., Hjelmstad, J., & Aarholt, E. (1995). Ground penetrating synthetic pulse radar: dynamic range and modes of operation. *Journal of Applied Geophysics, 33,* 7–14.

Jadoon, K. Z., Weihermüller, L., McCabe, M. F., Moghadas, D., Vereecken, H., & Lambot, S. (2015). Temporal monitoring of the soil freeze-thaw cycles over a snow-covered surface by using air-launched ground-penetrating radar. *Remote Sensing, 7*(9), 12041–12056.

Jol, H. M. (2009). *Ground Penetrating Radar: Theory and Applications* (pp. 534). Amsterdam: Elsevier.

Khamzin, A. K., Varnavina, A. V., Torgashov, E. V., Anderson, N. L., & Sneed, L. H. (2017). Utilization of air-launched ground penetrating radar (GPR) for pavement condition assessment. *Construction and Building Materials, 141,* 130–139. https://doi.org/10.1016/j.conbuildmat.2017.02.105.

Krellmann, Y., & Triltzsch, G. (2012). HERA-G—a new helicopter GPR based on gated stepped frequency technology. In *14th International conference on ground penetrating radar (GPR)* (pp. 4). June 4–8, 2012, Shanghai, China.

Lambot, S., Weihermüller, L., Huisman, J. A., Vereecken, H., Vanclooster, M., & Slob, E. C. (2006). Analysis of air-launched ground-penetrating radar techniques to measure the soil surface water content. *Water Resources Research, 42,* W11403. https://doi.org/10.1029/2006wr005097.

Langhammer, L., Rabenstein, L., Bauder, A., & Maurer, H. (2017). Ground-penetrating radar antenna orientation effects on temperate mountain glaciers. *Geophysics, 82*(3), H15–H24. https://doi.org/10.1190/GEO2016-0341.1.

Langhammer, L., Rabenstein, L., Schmid, L., Bauder, A., Grab, M., Schaer, P., et al. (2018). Glacier bed surveying with helicopter-

borne dual-polarization ground-penetrating radar. *Journal of Glaciology*. https://doi.org/10.1017/jog.2018.99.

Lehmann, F., & Green, A. G. (2000). Topographic migration of georadar data: implications for acquisition and processing. *Geophysics, 65*(3), 836–848. https://doi.org/10.1190/1.1444781.

Machguth, H., Eisen, O., Paul, F., & Hoelzle, M. (2006). Strong spatial variability of snow accumulation observed with helicopter-borne GPR on two adjacent Alpine glaciers. *Geophysical Research Letters, 33*(13), L13503. https://doi.org/10.1029/2006GL026576.

Melcher, N. B., Costa, J. E., Haeni, F. P., Cheng, R. T., Thurman, E. M., Buursink, M. K., et al. (2002). River discharge measurements by using helicopter-mounted radar. *Geophysical Research Letters, 29,* 41-1–41-4. https://doi.org/10.1029/2002gl015525.

Merz, K., Green, A. G., Buchli, T., Springman, S. M., & Maurer, H. (2015a). A new 3-D thin-skinned rock glacier model based on helicopter GPR results from the Swiss Alps. *Geophysical Research Letters, 42,* 4464–4472. https://doi.org/10.1002/2015GL063951.

Merz, K., Maurer, H. R., Buchli, T., Horstmeyer, H., Green, A. G., & Springman, S. M. (2015b). Evaluation of ground-based and helicopter ground-penetrating radar data acquired across an alpine rock glacier. *Permafrost and Periglacial Processes, 26,* 13–27. https://doi.org/10.1002/ppp.1836.

Moran, M. L., Greenfield, R. J., & Arcone, S. A. (2003). Modeling GPR radiation and reflection characteristics for a complex temperate glacier bed. *Geophysics, 68,* 559–565.

Negi, H. S., Thakur Snehmani, N. K., & Sharma, J. K. (2008). Estimation of snow depth and detection of buried objects using airborne Ground Penetrating Radar in Indian Himalaya. *Current Science, 94*(7), 865–870.

Nobes, D. C. (1999). The directional dependence of the Ground Penetrating Radar response on the accumulation zones of temperate alpine glaciers. *First Break, 17*(7), 249–259.

O'Neel, S., McGrath, D., Wolken, G. J., Whorton, E. N., Candela, S. G., Sass, L. C., McNeil, C. J., Baker, E. H., Peitzsch, E. H., Fagre, D. B., Clark, A. M., Florentine, C. E., Miller, Z. S., Christian, J. E., Christianson, K., Babcock, E. L., Loso, M. G., Arendt, A. A., Burgess, E. W., Gusmeroli, A. (2018). Raw ground penetrating radar data on North American glaciers (ver. 2.1, September 2018). US Geological Survey data release. https://doi.org/10.5066/f7m043g7.

Pfeffer, W., Arendt, A. A., Bliss, A., Bolch, T., Cogley, J., Gardner, A., et al. (2014). The Randolph glacier inventory: a globally complete inventory of glaciers. *Journal of Glaciology, 60*(221), 537–552. https://doi.org/10.3189/2014JoG13J176.

Plewes, L. A., & Hubbard, B. (2001). A review of the use of radio echo sounding in glaciology. *Progress in Physical Geography, 25*(2), 203–236.

Rückamp, M., & Blindow, N. (2012). King George Island ice cap geometry updated with airborne GPR measurements. *Earth System Science Data, 4,* 23–30. https://doi.org/10.5194/essd-4-23-2012.

Rutishauser, A., Maurer, H., & Bauder, A. (2016). Helicopter-borne ground-penetrating radar investigations on temperate alpine glaciers: A comparison of different systems and their abilities for bedrock mapping. *Geophysics, 81*(1), WA119–WA129. https://doi.org/10.1190/geo2015-0144.1.

Salvatore, M. C., Zanoner, T., Baroni, C., Carton, A., Banchieri, F. A., Viani, C., et al. (2015). The state of Italian glaicers: a snapshot of the 2006–2007 hydrological period. *Geografia Fisica e Dinamica Quaternaria, 38,* 175–198. https://doi.org/10.4461/GFDQ.2015.38.16.

Sen, M., Stoffa, P. L., Seifoullaev, R. K., & Fokkema, J. T. (2003). Numerical and Field Investigations of GPR: toward an Airborne GPR. *Subsurface Sensing Technologies and Applications, 4*(1), 41–60.

Siegert, M. J., Hindmarsh, R., Corr, H., Smith, A. M., Woodward, J., King, E. C., et al. (2004). Subglacial Lake Ellsworth: a candidate for in situ exploration in West Antarctica. *Geophysical Research Letters, 31,* L23403.

Smiraglia, C., & Diolaiuti, G. (2015). *Il Nuovo catasto dei Ghiacciai italiano*. Comitato Ev-K2-CNR (Ed.) Bergamo (pp. 400) (in Italian).

Steenson, B. O. (1951). *Radar methods for the exploration of glaciers.* Unpublished Ph.D. thesis. Pasedena, USA: Californian Institute of Technology.

Truss, S., Grasmueck, M., Vega, S., & Viggiano, D. A. (2007). Imaging rainfall drainage within the Miami oolitic limestone using high-resolution time-lapse ground penetrating radar. *Water Resources Research, 43*(3), W03405.

Urbini, S., Zirizzotti, A., Baskaradas, J. A., Tabacco, I. E., Cafarella, L., Senese, A., et al. (2017). Airborne radio echo sounding (RES) measures on alpine glaciers to evaluate ice thickness and bedrock geometry: preliminary results from pilot tests performed in the Ortles-Cevedale Group (Italian Alps). *Annals of Geophysics, 60*(2), G0226.

Vaughan, D. G., Corr, H. F. J., Doake, C. S. M., & Waddington, E. D. (1999). Distortion of isochronous layers in ice revealed by ground-penetrating radar. *Nature, 398,* 323–326. https://doi.org/10.1038/18653.

Watte, A. H., & Schmidt, S. J. (1962). Gross errors in height indication from pulsed radar altimeters operating over thick ice or snow. *Proceedings of the Institute of Radio Engineers, 50,* 1516–1520.

Wynn, R. B., Huvenne, V. A. I., Le Bas, T. P., Murton, B. J., Connelly, D., Bett, B. J., et al. (2014). Autonomous underwater vehicles (AUVs): their past, present and future contributions to the advancement of marine geosciences. *Marine Geology, 352,* 451–468.

(Received September 17, 2018, revised February 28, 2019, accepted April 11, 2019)